Reproducible chemostat cultures to eliminate eukaryotic viruses from fecal transplant material

Signe Adamberg[1], Torben Sølbeck Rasmussen[2], Sabina Brigitte Larsen[2], Dennis Sandris Nielsen[2], Kaarel Adamberg[1,3]

[1]Department of Chemistry and Biotechnology, Tallinn University of Technology, Akadeemia tee 15, Tallinn, Estonia

[2]Section of Microbiology and Fermentation, Department of Food Science, University of Copenhagen

[3]Center of Food and Fermentation Technologies, Mäealuse 2/4, 12618, Tallinn, Estonia

ABSTRACT

The effect of fecal microbiota transplantation (FMT) on various gut-related diseases is intensively investigated in clinical trials. In addition to bacteria, the gut microbiome also contains eukaryotic, archaeal, and bacterial viruses (bacteriophages, in short phages), which collectively is referred to, as the gut virome. Application of FMT in clinical studies is associated with a potential risk for the recipient of transferring infectious eukaryotic viruses or bacteria, despite strict screening procedure of the donor material. A safer and more targeted method to modulate the gut microbiota is therefore needed to extend the application width of FMT. Emerging evidence suggests that gut phages play a key role in maintaining a balanced gut microbiome as well as in FMT efficacy. Thus, a phageome from a cultured fecal donor microbiome may be a more efficient alternative to modulate the gut bacteriome than FMT. Here, we analyzed the dynamic changes of the viromes of mice cecal and human fecal cultures in chemostat cultures. Sequencing results showed that the relative abundance of eukaryotic viruses remarkably decreased during continuous cultivation, likely due to the lack of eukaryotic hosts. The corresponding phageome profiles showed dilution rate dependency, a reproducibility between biological replicates, and to maintain a high and stable diversity of phages although being different from the inoculum phageome. This proof-of-concept study may constitute the first step of developing therapeutic tools to target a broad spectrum of gut-related diseases and thereby replacing FMT with a safer phage-mediated therapy.

INTRODUCTION

Transplantation of fecal microbiota (FMT) have been successfully applied to treat especially recurrent *Clostridioides difficile* infections (rCDI) possibly through bacteriophage-mediated (bacterial viruses, in short phages) modulation of the GM landscape [1–4]. The fecal donor material used for FMT is screened for amongst other pathogenic bacteria and viruses prior FMT to ensure the safety. However,

34 this process is laborious and may only end up with 3% of the donor participants passing all safety steps
35 [5]. Fecal virome transplantation (FVT, sterile filtrated donor feces) have also shown promising
36 treatment efficiency against rCDI [2, 6] and in a recent preclinical CDI study [7]. An important
37 advantage of the FVT over FMT is the elimination of bacterial transfer as a potential threat. However,
38 there is still the risk of transferring disease-causing eukaryotic viruses even after the screening of
39 donor material for known pathogenic viruses as long-term effects of the most viruses are not yet
40 studied.

41 The interactions between gut bacteria and phages are complex and gut microbiome diversity is linked
42 to gut virome diversity, hence making the gut virome an important component in health and disease
43 [8, 9]. Microbiome abundances and diversity are predictive of virome richness and diversity [10] and
44 the number of virus-like particles (VLP) in feces has been estimated to be between 10^9 and 10^{10} VLP/g
45 [11–14]. The human gut virome is dominated by phages (over 97%) and only about one tenth of those
46 have been annotated until now [15]. There are several indications that viromes of the dysbiotic gut
47 microbiota differ from those of a healthy gut microbiota [16–18], however the causal links remain still
48 poorly understood. The healthy adult gut virome is highly personal and stable over time within each
49 individual [11, 19, 20]. Phages belonging to the order *Caudovirales* are the most dominant in the
50 human gut [8, 9, 21, 22]. The impact of phageome on the composition and function of the gut
51 microbiota has been suggested to have important consequences for health and outcome of FMT or
52 FVT treatments [2, 23–26].

53 While phages only infect bacterial and not eukaryotic cells, we aimed to develop methodologies to
54 produce active enteric phage communities with minimized amounts of eukaryotic viruses using two
55 different inocula; murine cecal and human fecal microbiota. Of which the chemostat propagated
56 murine gut virome ability to improve gut microbiota balance was evaluated in preclinical studies
57 representing animal models with distinct disease etiologies; CDI [7] and diet-induced obesity [27]. Our
58 recent studies highlighted the importance of dilution rate on the composition of fecal microbiota [28,
59 29]. The cultivation conditions and substrates were chosen to sustain the highest microbial diversity
60 based on previous knowledge. The dynamics and stability of the chemostat cultures were followed by
61 determination of bacterial and viral composition, growth characteristics and metabolic products. We
62 hypothesized that eukaryotic viruses would be washed out from the intestinal microbiota in
63 continuous *in vitro* culture due to the dilution effect. The dynamic changes of enteric phages in
64 chemostat cultures have not been reported earlier.

65

METHODS

Chemostat inocula

Chemostat cultivations were carried out with two different intestinal inocula of human and mouse origin, respectively. The human study was approved by Tallinn Medical Research Ethics Committee, Estonia (protocol no. 554). Fecal samples from seven healthy donors (age 19-37 years, Caucasian, three male and four female) were diluted five times, pooled in equal volumes and stored frozen at -80°C until use as described previously in Adamberg et al. [30]. Cecal content of mice from different vendors were pooled, as previously we have shown that mice from different vendors represents completely different gut microbiota profiles (both the bacterial and viral community) [31, 32]. In total 18 C57BL/6N male mice were purchased to harvest intestinal content for downstream applications. The mice were five weeks old at arrival and purchased from three vendors, represented by 6 C57BL/6NTac mice (Taconic, Lille Skensved, Denmark), 6 C57BL/6NRj mice (Janvier, Le Genest-Saint Isle, France), and 6 C57BL/6NCrl mice (Charles River, Sulzfeld, Germany) and ear marked at arrival. Animal housing was carried out at Section of Experimental Animal Models, University of Copenhagen, Denmark (Danish Animal Experimentation Act with the license ID: 2012-15-2934-00256), under the conditions as described previously [31]. For 13 weeks the mice were fed *ad libitum* low-fat diet (LF, Research Diets D12450J, USA) until termination at 18 weeks old and their body weight were measured every second week. To preserve the viability of the strict anaerobic bacteria, 6 mice from each vendor (in total 18 mice) were sacrificed by cervical dislocation and immediately transferred to a jar containing an anaerobic sachet (cat. no. AN0035A AnaeroGen, Thermo Fisher Scientific) and subsequently to an anaerobic chamber (containing ~93 % N_2, ~2 % H_2, ~5 % CO_2) at room temperature (Model AALC, Coy Laboratory Products, Grass Lake, Michigan, USA) where cecum content of the mice was sampled. Inside the anaerobic chamber, the samples were processed according to vendor (Janvier, Charles River and Taconic); weighted, suspended in an anoxic 1:1 mixture of PBS (NaCl 137 mM, KCl 2.7 mM, Na2HPO4 10 mM, KH2PO4 1.8 mM) and 50% glycerol and homogenized in BagPage® 100 mL filter bags (Interscience, Saint-Nom-la-Bretèche, France) with a laboratory stomacher (Stomacher 80, Seward, UK) at medium speed for 120 seconds. The cecum content from mice from all vendors were mixed, and the pooled cecum content was divided into 6 cryotubes ~ 0.5 g cecum content in each, one for each chemostat run. The samples were frozen at -80°C and shipped on dry ice with express delivery to Tallinn University of Technology, Estonia where the chemostat experiment were performed. The abovementioned processes are illustrated with a flow-diagram (Supplementary Fig. S1). All procedures regarding the handling of these animals used for donor materiel were carried out in accordance with the Directive 2010/63/EU and the Danish Animal Experimentation Act with the license ID: 2012-15-2934-00256.

100

101 **Growth medium**

102 The base medium was prepared in a 0.05 M potassium phosphate buffer containing amino acids,
103 mineral salts and vitamins as described previously [29]. Hemin (5 mg/L), menadione (0.5 mg/L), bile
104 salts (0.5 g/L), NaHCO3 (2.0 g/L), Tween-80 (0.5 g/L), Na-thioglycolate (0.5 g/L) and Cys-HCl (0.5 g/L,
105 freshly made in oxygen reduced water) were added to the base medium. Carbohydrate sources for
106 the human fecal (human) cultures were apple pectin (2.5 g/L, Sigma-Aldrich, USA) and porcine mucin
107 (2.5 g/L, Type II, Sigma Aldrich, USA). The carbohydrate sources were sterilized separately and added
108 to the medium before experiments. Carbohydrate sources and other components added to the
109 medium for murine (mouse) cultures were apple pectin (2 g/L, Sigma-Aldrich, USA), chickory inulin HP
110 (1 g/L, Orafti, Belgium), corn core xylan (2 g/L, TCI, Japan), corn starch (5 g/L, Sigma-Aldrich, USA),
111 larch wood arabinogalactan (2 g/L, TCI, Japan) and porcine mucin (4 g/L, Type II, Sigma Aldrich, USA),
112 acetic acid (0.3 g/L, Sigma-Aldrich, USA), tryptone (3 g/L, LABM, UK) and yeast extract (3 g/L, LABM,
113 UK) as described by Macfarlane et al. [33].

114

115 **Cultivation system and culture conditions**

116 The cultivation system described earlier [29] was used for human fecal and mice cecal cultures. Briefly,
117 the Biobundle cultivation system consisting of the ADI 1030 bio-controller and cultivation control
118 program "BioXpert" (Applikon, The Netherlands). The fermenter was equipped with sensors for pH,
119 pO_2, and temperature. Variable speed pumps for feeding and outflow were controlled by a chemostat
120 algorithm: D = F/V, where D is the dilution rate (1/h), F is the feeding rate (L/h), and V is the fermenter
121 working volume (L). pH was controlled by a 1M NaOH addition according to the pH setpoint. The
122 medium in the feeding bottle and the fermenter was flushed with sterile-filtered nitrogen gas (99.9%,
123 AS Linde Gas, Estonia) overnight before inoculation and throughout the cultivation to maintain
124 anaerobiosis. The culture volume was kept constant (600 ml for mouse and 300 ml for human
125 cultures). The temperature was kept at 36.6 °C. pH was kept constant at pH =6.4 for mouse and 7.0
126 for human cultures depending on the physiological pH of the host. The experimental scheme of mouse
127 cecal culture experiments is depicted in the Fig. 1. Three ml of the pooled cecal cultures were
128 inoculated into 600 ml medium to start the mouse experiments. The chemostat algorithm was started
129 15-20 hours after inoculation, which corresponds to the middle of the exponential growth phase of
130 the fecal culture. Three replicates were carried out with human and mouse inocula at two dilution
131 rates, 0.05 1/h (D_{low}) and 0.2 1/h (D_{high}), except for mouse cultures at D_{high} where two experiments
132 were performed. The stabilization time was five residence times in all experiments. On-line and at-line
133 parameters used for experiment control are depicted on the Supplementary Fig. S2.

134

135 **Analytical methods**

136 Samples from the outflow were collected on ice, centrifuged (14,000 g, 5 min, 4 °C) and stored
137 separately as pellets (at -80°C) and supernatants (at -20°C) until further analyses. For chromatographic
138 analyses, culture supernatants were filtered using AmiconR Ultra-10K Centrifugal Filter Devices, cut-
139 off 3 kDa according to the manufacturer's instructions (Millipore, USA). The concentrations of organic
140 acids (succinate, lactate, formate, acetate, propionate, isobutyrate, butyrate, isovalerate and valerate)
141 and ethanol were determined by high-performance liquid chromatography (HPLC, Alliance 2795
142 system, Waters, Milford, MA, USA), using BioRad HPX-87H column (Hercules, CA, USA) with isocratic
143 elution of 0.005 M H2SO4 at a flow rate of 0.5 mL/min and at 35 °C. Refractive index (RI) (model 2414;
144 Waters, USA) and UV (210 nm; model 2487; Waters, USA) detectors and analytical grade standards
145 were used for quantification of the substances. The detection limit for the method was 0.1 mM.

146 The composition of the gas outflow (H_2, CO_2, H_2S, CH_4, and N_2) was analyzed using an Agilent 490 Micro
147 GC Biogas Analyzer (Agilent 269 Technologies Ltd., USA) connected to a thermal conductivity detector.
148 The volume of the gas flow was regularly recorded using MilliGascounter (RITTER Apparatebau GMBH
149 & Co, Germany).

150 For gas metabolism, pathways involved in CO_2 or formate production were considered. Pyruvate can
151 be converted into acetyl-CoA via the ferredoxin pathway with CO_2 and potential H_2 formation or
152 pyruvate-formate-lyase pathway resulting in formate production. Hence, the gas data was calculated
153 per product involved in CO_2 formation assuming that two moles of CO_2 is formed in butyrate
154 production, one mole of CO_2 is formed in acetate, ethanol, and propionate formation, and one mole
155 of CO_2 is fixed in succinate formation.

156 The Redox potential of the growth medium and culture supernatant was measured by a pH/Redox
157 meter using an InLab®Redox electrode (Mettler Toledo, USA). The biomass dry weight was measured
158 gravimetrically from 10 ml culture by centrifugation (6,000 rpm, 20 min), washing the biomass with
159 distilled water and drying in an oven at 105°C for 20 h.

160

161 **Pre-processing of samples for separation of viruses and bacteria**

162 Culture and inoculum samples were included to investigate microbiome changes over time.
163 Separation of the viruses and bacteria from the culture/inoculum samples generated a pellet and
164 supernatant by centrifugation and 0.45 µm filtering as described previously [31], however, the volume
165 of culture/inoculum homogenate was adjusted to 5 mL SM buffer.

166

167 **Bacterial DNA extraction, sequencing and pre-processing of raw data**

168 Human bacteriome data have been previously published [29] but to minimize errors due to using
169 different data processing methods, human bacteriome sequences were reanalyzed using the same
170 pipeline as described above for analysis of mice samples. Bead-Beat Micro AX Gravity (mod.1) kit from
171 A&A Biotechnology (Gdynia, Poland) was used to extract bacterial DNA from the culture/fecal pellet
172 by following the instructions of the manufacturer. The final purified DNA was stored at -80ºC and the
173 DNA concentration was determined using Qubit HS Assay Kit (Invitrogen, Carlsbad, California, USA) on
174 the Qubit 4 Fluorometric Quantification device (Invitrogen, Carlsbad, California, USA). The bacterial
175 community composition was determined by NextSeq-based (Illumina) high-throughput sequencing
176 (HTS) of the 16S rRNA gene V3-region, as previously described [24]. Quality-control of reads, de-
177 replicating, purging from chimeric reads and constructing zOTU was conducted with the UNOISE
178 pipeline [34] and taxonomically assigned with Sintax [35] (not yet peer reviewed). Taxonomical
179 assignments were obtained using the EZtaxon for 16S rRNA gene database [36]. Code describing this
180 pipeline can be accessed in github.com/jcame/Fastq_2_zOTUtable. The average sequencing depth
181 after quality control (Accession: PRJEB58777, available at ENA) for the fecal 16S rRNA gene amplicons
182 was 60,719 reads (min. 11,961 reads and max. 198,197 reads).

183

184 **Viral RNA/DNA extraction, sequencing and pre-processing of raw data**

185 The sterile filtered culture/fecal supernatant was concentrated using centrifugal filters Centrisart with
186 a filter cut-off at 100 kDA (Sartorius) by centrifugation centrifuged at 1,500 x g at 4ºC
187 (dx.doi.org/10.17504/protocols.io.b2qaqdse). The viral DNA/RNA was extracted from the
188 culture/fecal supernatants with Viral RNA mini kit (Qiagen) as previously described [31]. Reverse
189 transcription was executed using the SuperScript VILO Master mix by following the instructions of the
190 manufacturer and subsequently cleaned with DNeasy blood and tissue kit (Qiagen) by only following
191 step 3-8 of the manufacturers standard protocol. In brief, the DNA/cDNA samples were mixed with
192 ethanol, bound to the silica filter, washed two times, and eluted with 40 µL elution buffer. Multiple
193 displacement amplification (MDA, to include ssDNA viruses) using GenomiPhi V3 DNA amplification
194 kit (Cytiva) and sequencing library preparation using Nextera XT kit was performed at previously
195 described [31], and send for sequencing using the NovaSeq platform (NovoGene). The average
196 sequencing depth of raw reads (Accession: PRJEB58787, available at ENA) for the fecal viral
197 metagenome was 22,701,135 reads (min. 342,022 reads and max. 203,403,294 reads. The raw reads
198 were trimmed from adaptors and the high-quality sequences (>95% quality) using Trimmomatic v0.35
199 [37] with a minimum size of 50 nt were retained for further analysis. High quality reads were de-
200 replicated and checked for the presence of PhiX control using BBMap (bbduk.sh)

201 (https://www.osti.gov/servlets/purl/1241166). Virus-like particle-derived DNA sequences were
202 subjected to within-sample de-novo assembly-only using Spades v3.13.1 [38] and the contigs with a
203 minimum length of 2,200 nt, were retained. Contigs generated from all samples were pooled and de-
204 replicated at 90% identity using BBMap (dedupe.sh). Prediction of viral contigs/genomes was carried
205 out using VirSorter2 [39] ("full" categories | dsDNAphage, ssDNA, RNA, Lavidaviridae, NCLDV |
206 viralquality ≥ 0.66), vibrant [40] (High-quality | Complete), and checkv [41] (High-quality | Complete).
207 Taxonomy was inferred by blasting viral ORF against viral orthologous groups (https://vogdb.org) and
208 the Lowest Common Ancestor (LCA) for every contig was estimated based on a minimum e-value of
209 $10e^{-5}$. Phage-host prediction was determined by blasting (85% identity) CRISPR spacers and tRNAs
210 predicted from >150,000 gut species-level genome bins (SGBs) [42, 43]. Following assembly, quality
211 control, and annotations, reads from all samples were mapped against the viral (high-quality) contigs
212 (vOTUs) using the bowtie2 [44] and a contingency-table of reads per Kbp of contig sequence per
213 million reads sample (RPKM) was generated, here defined as vOTU-table (viral contigs). Code
214 describing this pipeline can be accessed in github.com/jcame/virome_analysis-FOOD. Viral mock
215 communities (phage C2, T7, P35, MS2, Phi6, PhiX174, T4, and PMBT5) were used as positive controls
216 to evaluate if the library preparation and sequencing could detect ss/dsDNA and ss/dsRNA viruses
217 with a titer of ~10^6 PFU/mL from both pure phage culture as well as spiked fecal matrices.

218

219 **Bioinformatic analysis of bacterial and viral sequences**

220 Initially the dataset was purged for zOTU's/viral contigs, which were detected in less than 5% of the
221 samples, but the resulting dataset still maintained 99.5% of the total reads. Cumulative sum scaling
222 (CSS) [45] was applied for the analysis of beta-diversity to counteract that a few zOTU/viral contigs
223 represented a large fraction of count values, since CSS have been benchmarked with a high accuracy
224 for the applied metrics [46]. CSS normalization was performed using the R software using the
225 metagenomeSeq package [47]. R version 4.2.2 [48] was used for subsequent analysis and presentation
226 of data. The main packages used were phyloseq [49], vegan [50], deseseq 2 [51], ampvis2 [52], ggpubr,
227 and ggplot2 [53]. A-diversity analysis was based on raw read counts and statistics were based on
228 ANOVA. B-diversity was represented by Bray Curtis dissimilarity metrics and statistics were based on
229 PERMANOVA.

230

231 # RESULTS

232 With the aim of generating viromes depleted of eukaryotic viruses mouse cecal and human fecal
233 matter where propagated initially as batch cultures and subsequently in chemostat mode at two
234 different dilution rates (D_{low}, 0.05 1/h and D_{high}, 0.2 1/h) . The overall concept for both cultures (i.e

235 dilution rates, temperatures, and pH) was the same except for some differences in the media
236 composition. Most importantly, the total carbohydrate concentration was three times higher in the
237 medium for mouse-mimicking compared to that for the human-mimicking cultures (15.2 g/L vs 5 g/L,
238 respectively), to resemble the high content of complex carbohydrate in mice chow feed.
239
240 **Wash-out of eukaryotic viruses from chemostat cultures**
241 The relative abundance of eukaryotic viruses decreased already after batch phase and were almost
242 depleted after five residence times in chemostat of both mouse cecal and human fecal cultures (Fig.
243 2). At the same time, the bacterial virome maintained high diversity in the chemostat phase (Fig. 3
244 and Supplementary Fig. S3).
245 Both eukaryotic DNA viruses and phages were identified in both inocula (Fig. 3). RNA viruses
246 (*Leviviridae* and *Cystoviridae*) were found only in human cultures and their count in mouse cultures
247 remained below detection limit of virus particles (10^6 VLP/mL). The most abundant taxon of eukaryotic
248 viruses in mouse cultures was *Mimiviridae* and the abundances of other identified viral taxa
249 (*Herpesviridae* and *Parvoviridae*) were two magnitudes lower than *Mimiviridae*. Similarly, *Mimiviridae*
250 but also *Circoviridae* were the most abundant eukaryotic viruses in human cultures, however, their
251 relative abundance from all viruses was below 1%. Nearly half of the viruses remained unidentified in
252 both mouse and human cultures, which may comprise unknown eukaryotic viruses.
253
254 **Propagating reproducible viromes in chemostat cultures**
255 Chemostat experiments showed that bacterial and archaeal viruses were persistent to continuous
256 culturing of gut microbiota and showed the dilution rate specific patterns. Diversity of bacterial virome
257 was significantly related to the dilution rate (Fig. 4). Shannon index of virome of mouse cultures
258 remained high even at the end of low dilution rate chemostat while remarkable reduction of diversity
259 was observed at high dilution rate. In human cultures, no clear associations were seen between the
260 virome diversity and cultivation conditions although Shannon index of batch cultures tended to be
261 higher than that in chemostat cultures. However, Shannon indices of bacteriomes of human fecal
262 cultures were higher in chemostats than these in batch cultures (Supplementary Fig. S4). The main
263 archaeal viral taxon was *Bicaudavirus* and its abundance was relatively stable in batch and chemostat
264 modes in both mouse and human cultures, which indicated that archaeal hosts may have been
265 propagating.
266 When examining overall virome and bacteriome compositional patterns, Fig. 4 shows that inocula and
267 samples of batch, slow and fast chemostat clustered into distinct groups. Viromes of batch samples
268 were closer to these of inoculum samples as there were no outflow but also show persistence of

269 viruses in these conditions. More importantly, our results indicate good reproducibility of chemostat
270 experiments as clearly separated clusters of chemostat samples were observed. Similar distinct
271 clustering was observed also for the bacteriome (see below and Supplementary Fig. S4).
272
273 **Dilution rate influences the composition of viromes**
274 In mouse batch cultures more than 90% of viral taxa could be identified while in chemostats the
275 number of unidentified viruses increased up to 50% at both dilution rates. In the end of the batch
276 phase, the mouse culture was dominated by *Bacteroides*, lactobacilli and *Enterobacteriaceae*.
277 Correspondingly, the main taxa of viruses were *Microviridae* and *Siphoviridae* (Fig. 3), which include
278 many viruses related to *Escherichia* and lactobacilli [54, 55]. *Microviridae*, the most abundant taxa in
279 the inoculum decreased significantly already in the batch phase and were mostly washed out for the
280 end of fast chemostat. However, in slow chemostat (D_{low}), *Microviridae* were still present in noticeable
281 amounts by the end of experiment. Other prevalent taxa in the virome at low dilution rate were
282 *Myoviridae* and *Podoviridae*.
283 The most abundant vira in human inoculum were also *Microviridae* (more than 70%) followed by
284 *Siphoviridae* and *Podoviridae* while the amounts of unidentified viruses remained below 10%. During
285 the batch phase the relative abundance of *Microviridae* and other annotated phages decreased while
286 that of unidentified viruses increased several times compared to their proportions in the inocula. At
287 both dilution rates of chemostat cultures *Microviridae* were mostly washed out and largely replaced
288 by viruses from the family *Myoviridae*, *Podoviridae,* and *Siphoviridae*. *Myoviridae* and *Podoviridae*
289 were especially abundant at fast dilution rate.
290 The assembled viral contigs were used to predict bacterial hosts using databases of CRISPR-arrays and
291 tRNA profiles. According to 16S rRNA gene sequence data, the dominant taxa in the inoculum were
292 *Ruminococcaceae*, *Lachnospiraceae* and lactobacilli but in the end of batch phase *Bacteroides*,
293 *Lactobacillus*, *Escherichia* and *Enterobacter* (Fig. 5). In the chemostat cultures with high dilution rates
294 (D = 0.2 1/h), the abundance of these four genera remained high. The abundance of lactobacilli
295 decreased from 23% to 12% while *Bacteroides* and enterobacteria remained the most dominant taxa
296 (both more than 20 %) in the end of chemostat propagation. In chemostats with low diution rate
297 inoculated with mouse cecal matter, *Bifidobacterium*, *Bacteroides*, *Blautia* and an unidentified
298 *Ruminococcaceae* became dominant. At the same time *Lactobacillus* and *Escherichia* were washed out
299 while *Akkermansia*, *Intestinimonas* and an unidentified *Lachnospiraceae* took over their place. Based
300 on the virome host prediction analyses, the prevalence of *Bacteroides* related viruses decreased more
301 than five times at low dilution rate being negligible at the end of chemostat propagation
302 (Supplementary Fig. S4). Higher bacteriome diversity was reflected also in higher virome diversity.

303 There were viruses related to genera *Akkermansia*, *Blautia*, *Enterococcus* and *Lachnoclostridium*, but
304 viruses related to bifidobacteria and *Ruminococcaceae* were not detected (Supplementary Fig. S4).
305 Completely different patterns could be seen in chemostats inoculated with fecal matter of human
306 origin. These were dominated by *Escherichia* and *Enterococcus* in the end of batch phase. It can be
307 explained by the remarkable differences of the composition of human and mouse inocula although
308 the dominant bacterial taxa were similar. In steady state (end of chemostat), the composition of
309 cultured mouse and human microbiota were more similar. *Bacteroides*, enterobacteria, bifidobacteria
310 and *Clostridium* were abundant in both cultures at high dilution rate while dominance of several
311 *Lachnospiraceae*, *Faecalibacterium* and *Collinsella* was characteristic to human cultures only.
312 *Akkermansia* and *Ruminococcaceae* members were on the other hand characteristic of chemostats
313 inoculated with mouse cecal or human fecel matter run with low dilution rate. Virome host analysis
314 showed that human fecal matter inoculated cultures contained mainly viruses related to *Bacteroides*,
315 *Faecalibacterium* and *Prevotella* in the end of batch phase (Supplementary Fig. S4). The fast dilution
316 rate promoted propagation of viruses related to *Bacteroides* but also to *Parabacteroides* and
317 *Methanobrevibacter*. The latter was not detected in bacteriome analyses of 16S rRNA gene amplicon
318 sequences.
319
320 **Bacterial metabolites are in accordance with the composition of microbiota**
321 In mouse cecal content inoculated batch cultures, the major metabolic products were acetate and
322 lactate, comprising about 30 and 24 mol%, respectively, followed by formate, ethanol, succinate and
323 propionate (Fig. 6). This in accordance to abundance of lactobacilli, *Bacteroides, Enterobacteriaceae*
324 members, and *Bifidobacterium* in microbiota (Fig. 5). Butyrate was almost missing, and propionate
325 represented less than 5 % of total acids (Fig. 6).
326 Remarkable differences were seen in the end-product profiles of mouse cecal content inoculated
327 cultures at the tested two different dilution rates, D_{low} = 0.05 1/h and D_{high} = 0.2 1/h (Fig. 6). The highest
328 acetate production (61 ± 2 mol-% of total products) was observed at D_{low}, while lactic acid was not
329 detected indicating its complete consumption by butyric and/or propionic acid producers. Ethanol was
330 produced in comparable amount with butyrate and propionate (all around 10 mol-%). Production of
331 succinate was below 10 mol-% at D_{low} and the amount of formate was marginal (0.1 mol-%).
332 In mouse cecal content inoculated cultures, similar amounts of formate and CO_2 were produced at
333 D_{high} (0.49 ± 0.04 and 0.46 ± 0.06 mol-CO_2/mol-products, respectively) while at D_{low} formate was not
334 produced and CO_2 formation was 0.33 ± 0.03 mol-CO_2/mol-products indicating other pathways for CO_2
335 cycling. Hydrogen production was enhanced at D_{high} (0.19 ± 0.01 and 0.015 ± 0.002 mol-CO_2/mol-
336 products, at D_{high} and at D_{low}, respectively).

337 When comparing mouse and human cecal/fecal content inoculated cultures, overall gas production
338 patterns were similar at D_{high} but significantly different at D_{low}. Formation of carbon dioxide and
339 hydrogen at D_{high} were 0.57 ± 0.12 and 0.15 ± 0.08 mol-CO_2(or H_2)/mol-products, respectively. At D_{low},
340 about 12 % higher CO_2 production was observed. Production of hydrogen sulfide indicating
341 degradation of sulfur containing amino acids and sulphated mucins, differed remarkably between the
342 two tested types of inoculum. H_2S production was high in both cultures, especially in human fecal
343 matter inoculated cultures (1.3 ± 0.1 and 5.5 ± 0.5 mmol/gDW in mouse cecal content vs. human fecal
344 matter inoculated cultures) at D_{low} but almost negligible in mouse cecal content inoculated cultures at
345 D_{high} (0.33 ± 0.03 and 4.6 ± 0.4 mmol/gDW in mouse cecal and human fecal matter inoculated cultures,
346 respectively).
347

348 # DISCUSSION

349 **Reproducibility of the virome propagation**

350 Here we aimed to produce chemostat-propagated viromes depleted of eukaryotic viruses. Two
351 different inocula (mouse cecal and human fecal matter) were tested at two different dilution rates.
352 The median relative abundance of contigs of eukaryotic origin decreased from 0.8 % (mouse cecal
353 culture) or 0.6 % (human fecal culture) to less than detectable amounts after five residence times in
354 chemostat cultivation. Interestingly, the virome appeared to be reproducible in parallel runs and both
355 the bacteriome and the virome approached equilibrium after five residence times. Thus, indicating
356 that extended time of the chemostat process to remove all eukaryotic viral particles would be
357 expected to maintain a similar virome profile as a shorter time for fermentation, and thereby providing
358 a safe and potential effective phage-mediated gut microbiota modulation tool to investigate or treat
359 gut-associated diseases.
360 There are very few data available concerning virus profiles of continuous cultures. However, the
361 composition of the virome would be expected to be reflected by the bacteriome profile due to their
362 inherent host-phage relationship. Interestingly, the relative abundances of phages did not correspond
363 to their host bacteria in the bacteriome as seen from Figs. 3 and 5. In general, *Podoviruses* and
364 *Myoviruses* have virulent lifestyle while *Siphoviruses* are lysogenic. In our study *Siphoviridae* was the
365 dominant viral family in both mouse cecal and human fecal inoculated cultures, whilst *Podoviridae*
366 and *Myoviridae* were abundantly present in the human fecal chemostat culture with high dilution rate.
367 This confirms that both lysogenic and virulent phages can be propagated in continuous cultures as
368 shown also by Santiago-Rodriquez et al. [56].

369 Previously, we have shown that chemostat can be used to produce reproducible bacterial consortia
370 from human fecal cultures [29]. In this study we confirmed this phenomenon on mice cecal cultures
371 and showed also that chemostat can be used to produce reproducible viromes.
372
373 **Dilution rate effects**
374 Dilution rate is a critical factor that determines the composition and metabolism of the chemostat
375 propagated bacteria [33]. This would be in line with the human gut transit time (a sort of "dilution
376 rate") being highly correlated to the gut microbiota diversity and composition [57, 58]. Dilution rates
377 0.05 and 0.2 1/h denote the fast growth in cecum and slow grow in the colon [28]. Microbial
378 metabolism directs the cross feeding between different community members and its changes affects
379 the overall metabolic patterns and composition of the consortium. As an example, *Akkermansia*, a
380 bacterium related to lower inflammatory response in the colon [59]. was a dominant species in both
381 mouse and human cultures at low dilution rate (0.05 1/h). On the other side the relative abundance
382 of butyric acid producers (species of *Lachnospiraceae*) were enhanced by high dilution rate (0.2 1/h)
383 [29]. In slow growing mouse cecal matter inoculated cultures (D_{low} = 0.05 1/h) higher diversity of the
384 bacteriome as well as phageome was obtained similar to what has also been reported for human fecal
385 matter inoculated chemostats by Asnicar et al. [58]. Thus, D_{low} in other words appear appropriate to
386 produce diverse microbiomes and phageomes from mouse cecal matter inoculated cultures. The
387 growth of *Enterobacteriaceae* and viruses predicted to have *Enterobacteriaceae* as host was
388 remarkably supported by fast dilution (D_{high} = 0.2 1/h) in mouse cecal matter inoculated chemostat-
389 fermentations.
390
391 **Chemostat propagation of active virome for in vivo trials**
392 The chemostat approach showed promising results for propagation of virome with minimal content
393 of eukaryotic viruses [7, 27]. In medical practice fecal microbiota transplantation (FMT) allows
394 modification of the intestinal microbiota. Although FMT has been shown safe and effective in a
395 immunocompromised CDI cohort [60], for these patients FMT is associated with several threats due
396 to transfer of virulent microbes and viruses [61]. To overcome these potential risks, continuous
397 cultivation of the fecal inoculum can be used to diminish the load of eukaryotic viruses by dilution,
398 since the environment in the chemostat is adjusted to only allow the propagation of bacteria and
399 phage communities, while eukaryotic hosts are absent. During continuous growth over five volumes
400 the bacterial and viral community reaches a stabilized composition that depend on the cultivation
401 conditions (e.g dilution rate, pH, substrates).
402

403 In conclusion, we showed that chemostat cultivation has potential as a method to generate mouse
404 cecal and human fecal phageome with minimal content of eukaryotic viruses. The phage populations
405 can be used in transplantation experiments after removing all bacteria. Using the conditions tested
406 here, the number of eukaryotic viruses can be decreased by more than hundred times of the initial
407 load.
408

409 # References

410 1. Fujimoto K, Kimura Y, Allegretti JR, Yamamoto M, Zhang Y, Katayama K, et al. Functional
411 Restoration of Bacteriomes and Viromes by Fecal Microbiota Transplantation.
412 *Gastroenterology* 2021; **160**: 2089–2102.
413 2. Ott SJ, Waetzig GH, Rehman A, Moltzau-Anderson J, Bharti R, Grasis JA, et al. Efficacy of
414 Sterile Fecal Filtrate Transfer for Treating Patients With Clostridium difficile Infection.
415 *Gastroenterology* 2017; **152**: 799-811.e7.
416 3. Petrof EO, Gloor GB, Vanner SJ, Weese SJ, Carter D, Daigneault MC, et al. Stool substitute
417 transplant therapy for the eradication of Clostridium difficile infection: 'RePOOPulating' the
418 gut. *Microbiome* 2013; **1**: 1–12.
419 4. Zuo T, Wong SH, Lam K, Lui R, Cheung K, Tang W, et al. Bacteriophage transfer during faecal
420 microbiota transplantation in Clostridium difficile infection is associated with treatment
421 outcome. *Gut* 2018; **67**: 634–643.
422 5. Kassam Z, Dubois N, Ramakrishna B, Ling K, Qazi T, Smith M, et al. Donor Screening for Fecal
423 Microbiota Transplantation. *N Engl J Med* 2019; **381**: 2070–2072.
424 6. Kao D, Roach B, Walter J, Lobenberg R, Wong K. EFFECT OF LYOPHILIZED STERILE FECAL
425 FILTRATE VS LYOPHILIZED DONOR STOOL ON RECURRENT CLOSTRIDIUM DIFFICILE INFECTION
426 (RCDI): PRELIMINARY RESULTS FROM A RANDOMIZED, DOUBLE-BLIND PILOT STUDY. *J Can*
427 *Assoc Gastroenterol* 2019.
428 7. Rasmussen TS, Forster S, Larsen SB, Von Münchow ASGL, Tranæs KD, Brunse A, et al. Fecal
429 viromes depleted of enveloped viruses efficiently treats Clostridioides difficile-associated
430 diarrhea in a murine model. *bioRxiv* 2023.
431 8. Cao Z, Sugimura N, Burgermeister E, Ebert MP, Zuo T, Lan P. The gut virome: A new
432 microbiome component in health and disease. *eBioMedicine* 2022; **81**: 104113.
433 9. Tiamani K, Luo S, Schulz S, Xue J, Costa R, Khan Mirzaei M, et al. The role of virome in the
434 gastrointestinal tract and beyond. *FEMS Microbiol Rev* 2022; **46**: 1–12.
435 10. Corzo-martinez M, García-campos G, Montilla A, Moreno FJ. Tofu whey permeate is an
436 efficient source to enzymatically produce prebiotic fructooligosaccharides and novel

437 fructosylated # -galactosides. *J Agric Food Chem* 2016.
438 11. Shkoporov AN, Clooney AG, Sutton TDS, Ryan FJ, Daly KM, Nolan JA, et al. The Human Gut
439 Virome Is Highly Diverse, Stable, and Individual Specific. *Cell Host Microbe* 2019; **26**: 527-
440 541.e5.
441 12. Shkoporov AN, Hill C. Bacteriophages of the Human Gut: The "Known Unknown" of the
442 Microbiome. *Cell Host Microbe* 2019; **25**: 195–209.
443 13. Lepage P, Colombet J, Marteau P, Sime-Ngando T, Doré J, Leclerc M. Dysbiosis in
444 inflammatory bowel disease: A role for bacteriophages? *Gut* 2008; **57**: 424–425.
445 14. Hoyles L, McCartney AL, Neve H, Gibson GR, Sanderson JD, Heller KJ, et al. Characterization of
446 virus-like particles associated with the human faecal and caecal microbiota. *Res Microbiol*
447 2014; **165**: 803–812.
448 15. Gregory AC, Zablocki O, Zayed AA, Howell A, Bolduc B, Sullivan MB. The Gut Virome Database
449 Reveals Age-Dependent Patterns of Virome Diversity in the Human Gut. *Cell Host Microbe*
450 2020; **28**: 724-740.e8.
451 16. Norman JM, Handley SA, Baldridge MT, Droit L, Liu CY, Keller BC, et al. Disease-specific
452 alterations in the enteric virome in inflammatory bowel disease. *Cell* 2015; **160**: 447–460.
453 17. Tao Z. Unveiling the gut virome in human health and diseases. *Int J Clin Virol* 2018; **2**: 001–
454 003.
455 18. Clooney AG, Sutton TDS, Shkoporov AN, Holohan RK, Daly KM, O'Regan O, et al. Whole-
456 Virome Analysis Sheds Light on Viral Dark Matter in Inflammatory Bowel Disease. *Cell Host*
457 *Microbe* 2019; **26**: 764-778.e5.
458 19. Manrique P, Bolduc B, Walk ST, Van Oost J Der, De Vos WM, Young MJ. Healthy human gut
459 phageome. *Proc Natl Acad Sci U S A* 2016; **113**: 10400–10405.
460 20. Minot S, Sinha R, Chen J, Li H, Keilbaugh SA, Wu GD, et al. The human gut virome: Inter-
461 individual variation and dynamic response to diet. *Genome Res* 2011; **21**: 1616–1625.
462 21. Spencer L, Olawuni B, Singh P. Gut Virome: Role and Distribution in Health and
463 Gastrointestinal Diseases. *Front Cell Infect Microbiol* 2022; **12**: 1–11.
464 22. Broecker F, Russo G, Klumpp J, Moelling K. Stable core virome despite variable microbiome
465 after fecal transfer. *Gut Microbes* 2017; **8**: 214–220.
466 23. Brunse A, Deng L, Pan X, Hui Y, Castro-Mejía JL, Kot W, et al. Fecal filtrate transplantation
467 protects against necrotizing enterocolitis. *ISME J* 2022; **16**: 686–694.
468 24. Beller L, Deboutte W, Vieira-Silva S, Falony G, Tito RY, Rymenans L, et al. The virota and its
469 transkingdom interactions in the healthy infant gut. *Proc Natl Acad Sci U S A* 2022; **119**.
470 25. Rasmussen TS, Mentzel CMJ, Kot W, Castro-Mejía JL, Zuffa S, Swann JR, et al. Faecal virome

471 transplantation decreases symptoms of type 2 diabetes and obesity in a murine model. *Gut*
472 2020; **69**: 2122–2130.
473 26. Rasmussen TS, Koefoed AK, Jakobsen RR, Deng L, Castro-Mejia JL, Brunse A, et al.
474 Bacteriophage-mediated manipulation of the gut microbiome-promises and presents
475 limitations. *FEMS Microbiol Rev* 2020; **44**: 507–521.
476 27. Mao X, Larsen SB, Zachariassen LSF, Brunse A, Adamberg S, Castro Mejia JL, et al. A
477 reproducible enteric phage community improves blood glucose regulation in an obesity
478 mouse model. *bioRxiv* 2023.
479 28. Adamberg K, Adamberg S. Selection of fast and slow growing bacteria from fecal microbiota
480 using continuous culture with changing dilution rate. *Microb Ecol Health Dis* 2018; **29**:
481 1549922.
482 29. Adamberg K, Raba G, Adamberg S. Use of Changestat for Growth Rate Studies of Gut
483 Microbiota. *Front Bioeng Biotechnol* 2020; **8**: 1–12.
484 30. Adamberg K, Tomson K, Talve T, Pudova K, Puurand M, Visnapuu T, et al. Levan enhances
485 associated growth of Bacteroides, Escherichia, Streptococcus and Faecalibacterium in fecal
486 microbiota. *PLoS One* 2015.
487 31. Rasmussen TS, de Vries L, Kot W, Hansen LH, Castro-Mejía JL, Vogensen FK, et al. Mouse
488 vendor influence on the bacterial and viral gut composition exceeds the effect of diet. *Viruses*
489 2019; **11**.
490 32. Rasmussen TS, Jakobsen RR, Castro-Mejía JL, Kot W, Thomsen AR, Vogensen FK, et al. Inter-
491 vendor variance of enteric eukaryotic DNA viruses in specific pathogen free C57BL/6N mice.
492 *Res Vet Sci* 2021; **136**: 1–5.
493 33. Macfarlane GT, Macfarlane S, Gibson GR. Validation of a Three-Stage Compound Continuous
494 Culture System for Investigating the Effect of Retention Time on the Ecology and Metabolism
495 of Bacteria in the Human Colon. *Microb Ecol* 1998; **44**: 180–187.
496 34. Edgar RC. Updating the 97% identity threshold for 16S ribosomal RNA OTUs. *Bioinformatics*
497 2018; **34**: 2371–2375.
498 35. Edgar R. SINTAX: a simple non-Bayesian taxonomy classifier for 16S and ITS sequences.
499 *bioRxiv* 2016; 074161.
500 36. Kim OS, Cho YJ, Lee K, Yoon SH, Kim M, Na H, et al. Introducing EzTaxon-e: A prokaryotic 16s
501 rRNA gene sequence database with phylotypes that represent uncultured species. *Int J Syst*
502 *Evol Microbiol* 2012; **62**: 716–721.
503 37. Bolger AM, Lohse M, Usadel B. Trimmomatic: A flexible trimmer for Illumina sequence data.
504 *Bioinformatics* 2014; **30**: 2114–2120.

505 38. Bankevich A, Nurk S, Antipov D, Gurevich AA, Dvorkin M, Kulikov AS, et al. SPAdes: A new
506 genome assembly algorithm and its applications to single-cell sequencing. *J Comput Biol*
507 2012; **19**: 455–477.
508 39. Guo J, Bolduc B, Zayed AA, Varsani A, Dominguez-Huerta G, Delmont TO, et al. VirSorter2: a
509 multi-classifier, expert-guided approach to detect diverse DNA and RNA viruses. *Microbiome*
510 2021; **9**: 1–13.
511 40. Kieft K, Zhou Z, Anantharaman K. VIBRANT: Automated recovery, annotation and curation of
512 microbial viruses, and evaluation of viral community function from genomic sequences.
513 *Microbiome* 2020; **8**: 1–23.
514 41. Nayfach S, Camargo AP, Schulz F, Eloe-Fadrosh E, Roux S, Kyrpides NC. CheckV assesses the
515 quality and completeness of metagenome-assembled viral genomes. *Nat Biotechnol* 2021;
516 **39**: 578–585.
517 42. Pasolli E, Asnicar F, Manara S, Zolfo M, Karcher N, Armanini F, et al. Extensive Unexplored
518 Human Microbiome Diversity Revealed by Over 150,000 Genomes from Metagenomes
519 Spanning Age, Geography, and Lifestyle. *Cell* 2019; **176**: 649-662.e20.
520 43. Castro-Mejía JL, Khakimov B, Aru V, Lind M V., Garne E, Paulová P, et al. Gut Microbiome and
521 Its Cofactors Are Linked to Lipoprotein Distribution Profiles. *Microorganisms* 2022; **10**: 1–15.
522 44. Langmead B, Salzberg SL. Fast gapped-read alignment with Bowtie 2. *Nat Methods* 2012; **9**:
523 357–359.
524 45. Paulson JN, Colin Stine O, Bravo HC, Pop M. Differential abundance analysis for microbial
525 marker-gene surveys. *Nat Methods* 2013; **10**: 1200–1202.
526 46. Weiss S, Xu ZZ, Peddada S, Amir A, Bittinger K, Gonzalez A, et al. Normalization and microbial
527 differential abundance strategies depend upon data characteristics. *Microbiome* 2017; **5**: 1–
528 18.
529 47. Paulson J. metagenomeSeq: Statistical analysis for sparse high-throughput sequencing.
530 *BioconductorJp* 2014; 1–20.
531 48. Team RC. R Core TeamR: A language and environment for statistical computing. R Foundation
532 for Statistical Computing, Vienna, Austria. 2018.
533 49. McMurdie PJ, Holmes S. Phyloseq: An R Package for Reproducible Interactive Analysis and
534 Graphics of Microbiome Census Data. *PLoS One* 2013; **8**.
535 50. Philip D. Computer program review VEGAN , a package of R functions for community ecology.
536 *J Veg Sci* 2003; **14**: 927–930.
537 51. Love MI, Huber W, Anders S. Moderated estimation of fold change and dispersion for RNA-
538 seq data with DESeq2. *Genome Biol* 2014; **15**: 1–21.

539 52. Andersen KS, Kirkegaard RH, Karst SM, Albertsen M. ampvis2: An R package to analyse and
540 visualise 16S rRNA amplicon data. *bioRxiv* 2018; 10–11.
541 53. Wickham H. Ggplot2. *Wiley Interdiscip Rev Comput Stat* 2011; **3**: 180–185.
542 54. Niu YD, McAllister TA, Nash JHE, Kropinski AM, Stanford K. Four Escherichia coli O157:H7
543 phages: A new bacteriophage genus and taxonomic classification of T1-like phages. *PLoS One*
544 2014; **9**.
545 55. Marcó MB, Garneau JE, Tremblay D, Quiberoni A, Moineau S. Characterization of two virulent
546 phages of Lactobacillus plantarum. *Appl Environ Microbiol* 2012; **78**: 8719–8734.
547 56. Santiago-Rodriguez TM, Ly M, Daigneault MC, Brown IHL, McDonald JAK, Bonilla N, et al.
548 Chemostat culture systems support diverse bacteriophage communities from human feces.
549 *Microbiome* 2015; **3**: 58.
550 57. Müller M, Hermes GDA, Canfora EE, Smidt H, Masclee AAM, Zoetendal EXG, et al. Distal
551 colonic transit is linked to gut microbiota diversity and microbial fermentation in humans
552 with slow colonic transit. *Am J Physiol - Gastrointest Liver Physiol* 2020; **318**: G361–G369.
553 58. Asnicar F, Leeming ER, Dimidi E, Mazidi M, Franks PW, Al Khatib H, et al. Blue poo: Impact of
554 gut transit time on the gut microbiome using a novel marker. *Gut* 2021; **70**: 1665–1674.
555 59. de Vos WM. Microbe profile: Akkermansia muciniphila: A conserved intestinal symbiont that
556 acts as the gatekeeper of our mucosa. *Microbiol (United Kingdom)* 2017; **163**: 646–648.
557 60. Suchman K, Luo Y, Grinspan A. Fecal Microbiota Transplant for Clostridioides Difficile
558 Infection Is Safe and Efficacious in an Immunocompromised Cohort. *Dig Dis Sci* 2022; **67**:
559 4866–4873.
560 61. Shogbesan O, Poudel DR, Victor S, Jehangir A, Fadahunsi O, Shogbesan G, et al. A Systematic
561 Review of the Efficacy and Safety of Fecal Microbiota Transplant for Clostridium difficile
562 Infection in Immunocompromised Patients. *Can J Gastroenterol Hepatol* 2018; **2018**.
563

564 # Figures

565

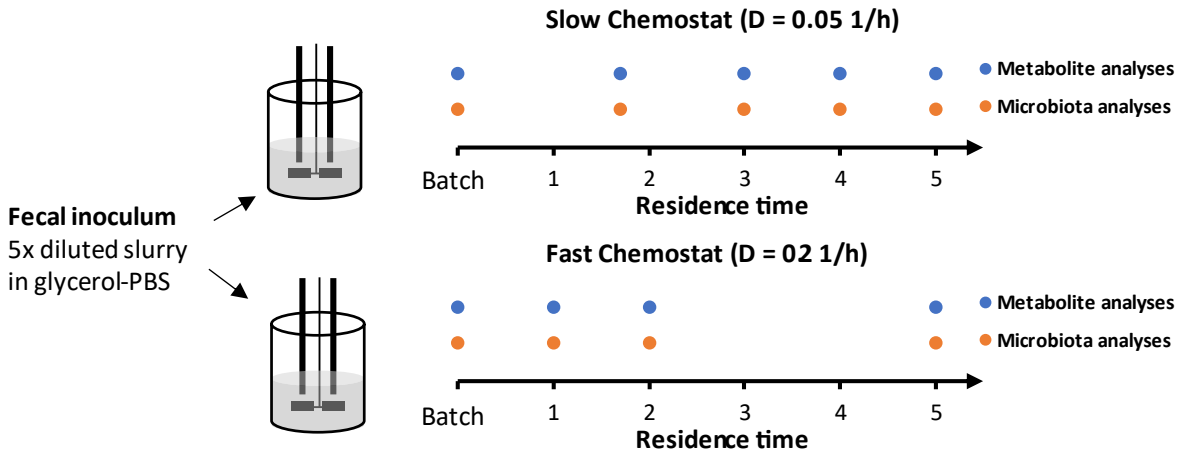

Fig. 1. The experimental setup of chemostat cultivations of mice cecal culture. At start one percent of five times diluted cecal content was inoculated into each bioreactor and batch growth was carried out 23 h followed by chemostat mode up to 5 residential times. Colored dots indicate the sampling points for metabolite and microbiota (16S rRNA gene amplicon and virome sequencing) analyses. Similar setup was also used for human fecal cultures [29].

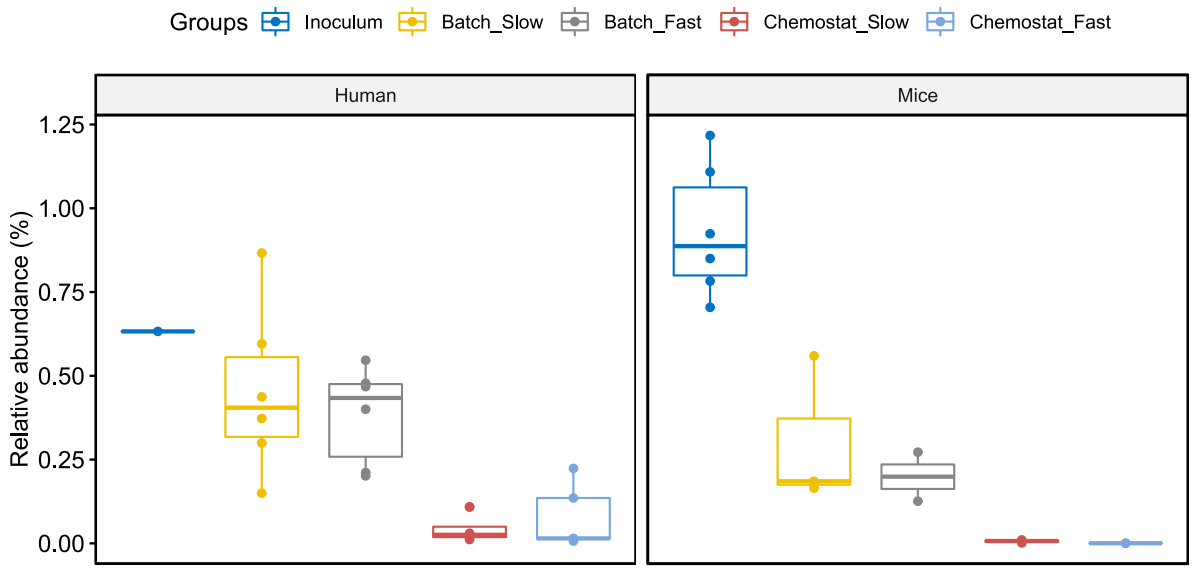

Fig. 2. Chemostat propagation of cecal/ fecal inocula leads to depletion of eukaryotic viruses. Relative abundance indicates the number of eukaryotic viral contigs from the total viral contigs in the inocula, batch and chemostat samples of human fecal and mouse cecal culture.

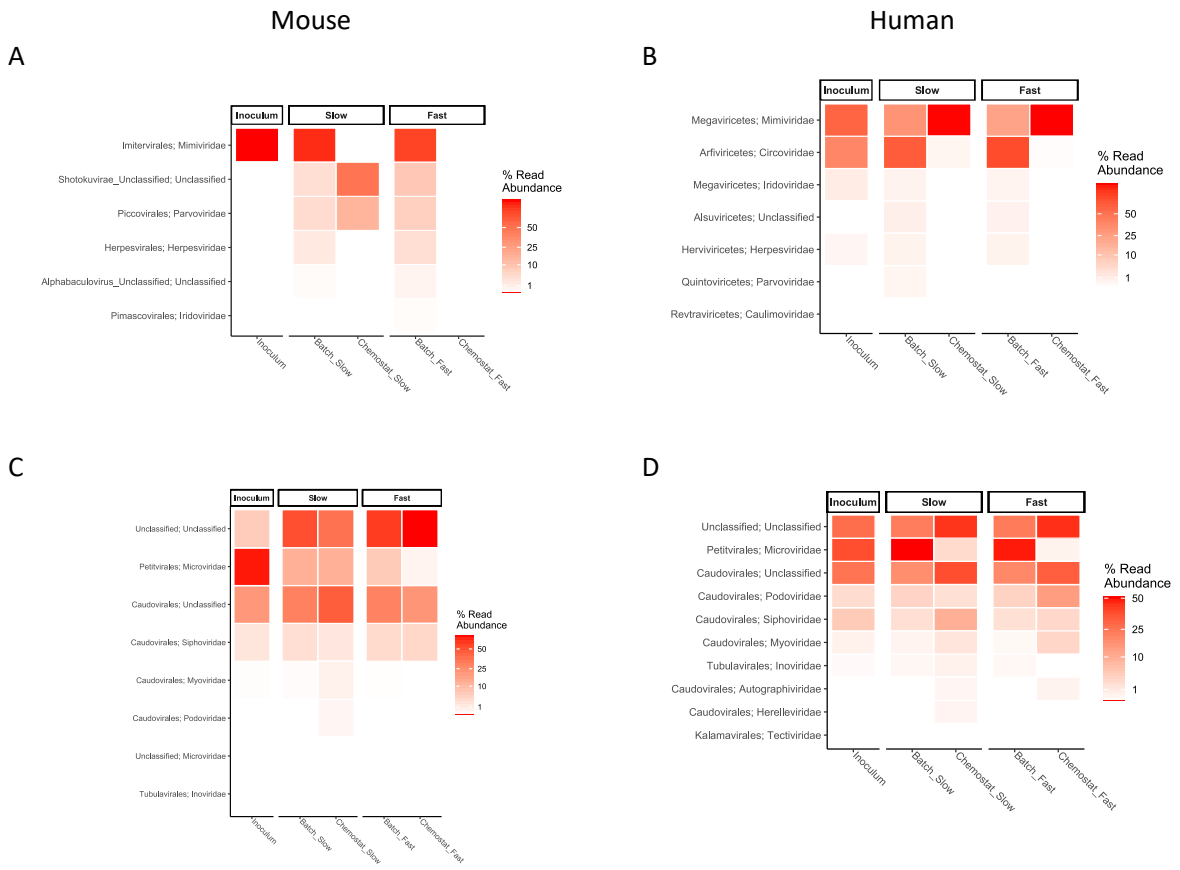

Fig. 3. Diversity of prokaryotic viruses during chemostat propagation of mouse cecal/ human fecal inocula. Depletion of eukaryotic viral families and enrichment of bacterial viral families from batch to stabilized chemostat cultures (A and C – mouse cecal samples, B and D – human fecal samples) presented as heatmaps. Color intensity indicates the relative abundance of eukaryotic (A, B) or prokaryotic (C, D) viral contigs from total eukaryotic or prokaryotic viral contigs, respectively. 'Slow' and 'Fast' indicate the dilution rates used in the chemostat (D_{low} 0.05 and D_{high} 0.2 1/h, respectively).

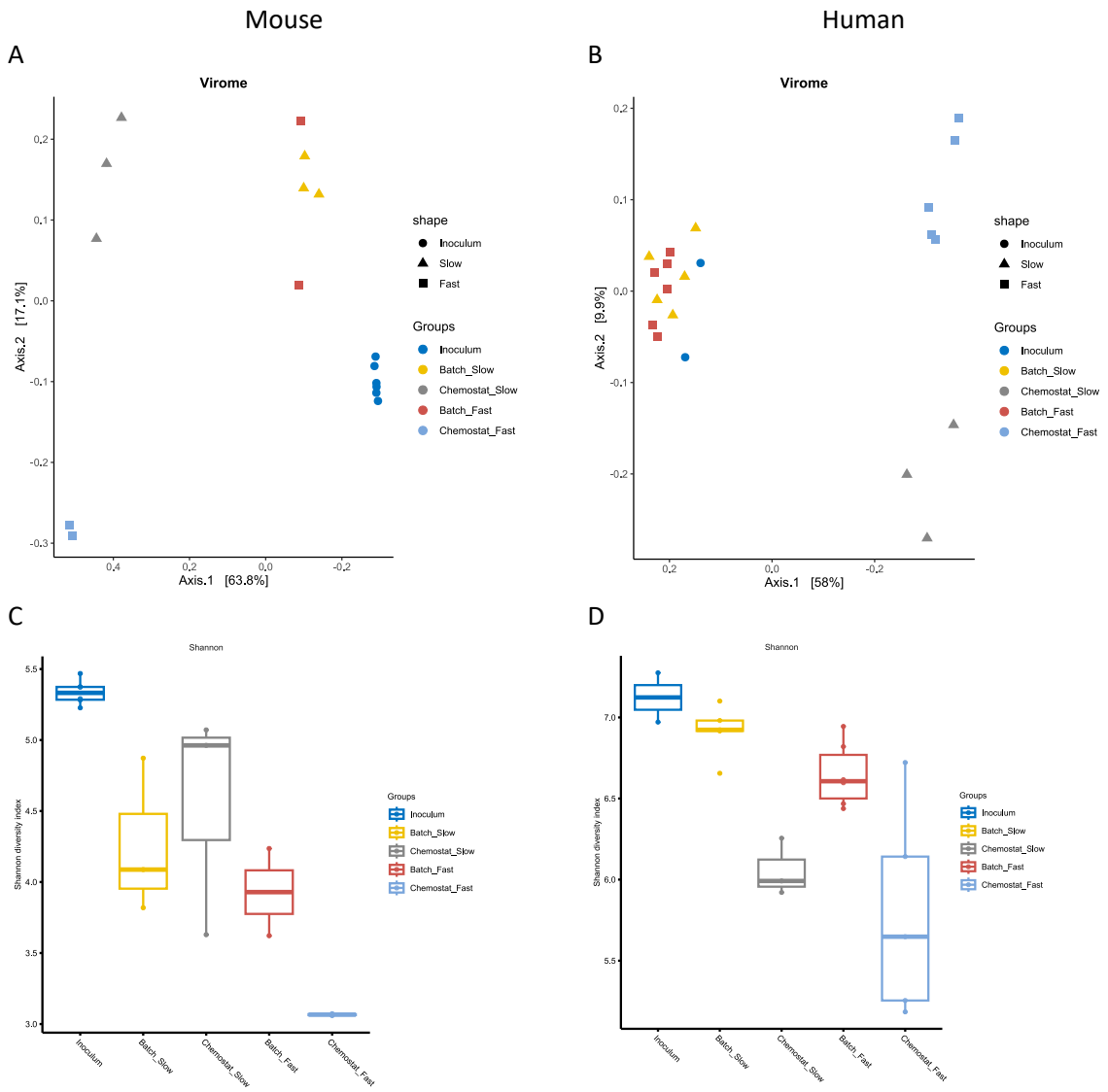

585

586 Fig. 4. Chemostat propagation of fecal inocula at different dilution rates leads to viromes with
587 reproducible compositon shown by beta diversity (A, B) and diverse viral community shown by
588 Shannon index (C, D). Samples from inoculum, batch and chemostat cultures of mouse cecal (A, C) and
589 human fecal (B, D) cultures are shown. 'Slow' and 'fast' in the column names indicate the dilution rate
590 used in the chemostat (D_{low} 0.05 and D_{high} 0.2 1/h, respectively). Beta diversity and Shannon indices of
591 bacteriomes are shown on the Supplementary Fig. S4.

592

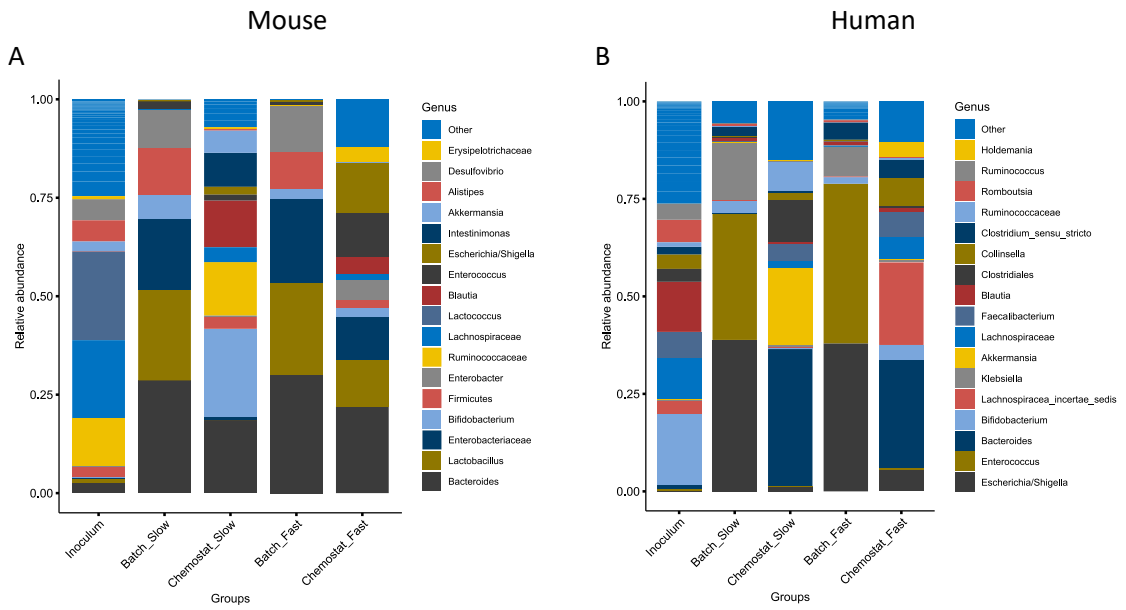

Fig. 5. Bacteriome composition of mice cecal (A) and human fecal cultures (B) after batch and chemostat propagation. 'Slow' and 'fast' in the column names indicate the dilution rate used in the chemostat (D_{low} 0.05 and D_{high} 0.2 1/h, respectively).

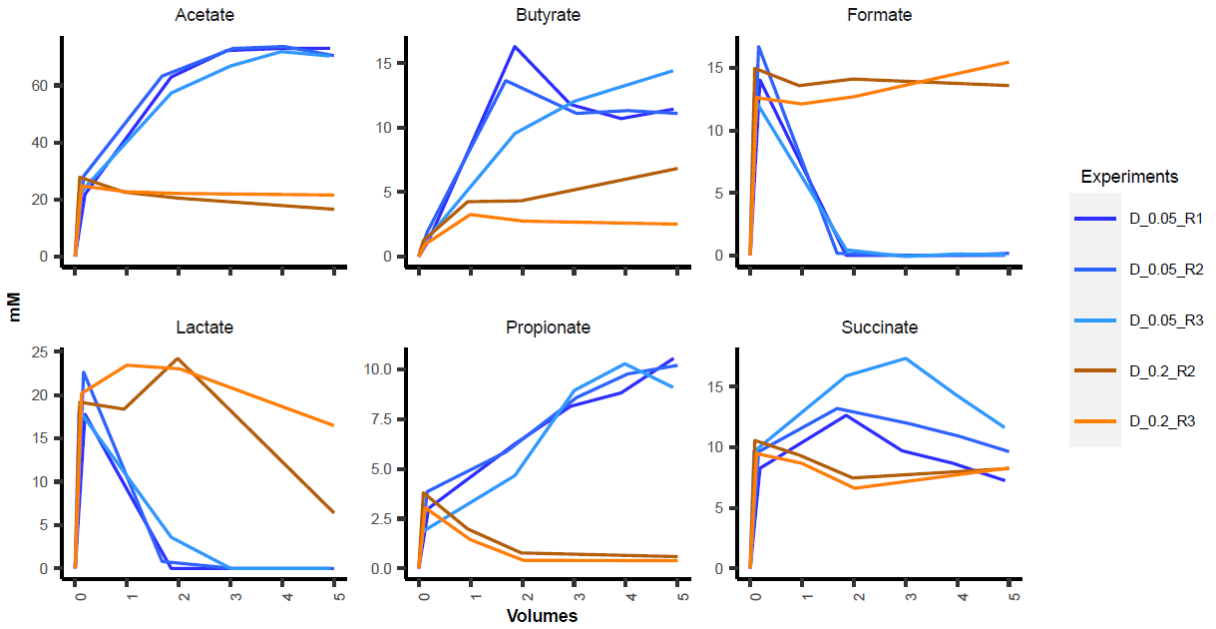

Fig. 6. Reproducibility of metabolite dynamics of chemostat propagated mouse cecal cultures at two dilution rates. Metabolite concentrations are shown in millimoles in relation to residence time ('Volumes' on x-scale). Low dilution rate (D = 0.05 1/h) is indicated with blue lines and high dilution rate (D = 0.2 1/h) with brown-orange lines. R indicates the number of replicate.